Electronic Supplementary Material (ESI) for Polymer Chemistry.


Supplementary Information

# Self-Healing Behaviour of Furan-Maleimide Poly(ionic liquid) Covalent Adaptable Networks

Katelyn M. Lindenmeyer, R. Daniel Johnson and Kevin M. Miller*

Department of Chemistry, Murray State University, Murray, KY 42071.

**Materials.** All chemicals were purchased from Sigma-Aldrich or Acros Organics and were used as received without further purification unless otherwise stated in the below procedures. An ELGA Purelab® Ultra filtration device produced ultrapure water having a resistivity of 18 MΩ-cm. The syntheses of 1,1′-(1,6-hexanediyl)bisimidazole,[1] furan-protected *N*-(4-bromobutyl)maleimide **1**[2] and TMPT-FUR[3] have been previously described elsewhere.

**Monomer Characterization.** $^{1}H$ and $^{13}C$ NMR spectra were obtained on a JEOL-ECS 400 MHz spectrometer and reported chemical shift values were referenced to residual solvent signals (DMSO-$d_6$: $^{1}H$, 2.50 ppm; $^{13}C$, 39.52 ppm). Elemental analyses (5 replicates for each polymer) were completed on a Perkin-Elmer 2400 CHNS/O Series II Elemental Analyzer. Residual bromide [Br] concentrations in monomers **4** and **7** were determined using ion chromatography (ICS-1100, Dionex) with an eluent concentration of 4.5 mN $CO_3^{2-}$/1.4 mM $HCO^{3-}$ and a flow rate of 1.2 mL/min with a cupressor current of 31 mA. Calibration with a set of aqueous standards prepared via serial dilution of a 1000 ppm [Br] stock solution (from sodium bromide, Aldrich, > 99.99 %). Each monomer was first dissolved in 1 mL of acetonitrile followed by injection. Residual [Br] was found to be less than 0.01 % *w*/*w*.

**Polymer Characterization.** For FTIR characterization, a Perkin-Elmer Spectrum Two™ FTIR Spectrometer in transmission mode was used to record spectra. The desired peaks ($cm^{-1}$ resolution, 48 scans) were followed and analyzed using the PerkinElmer Spectrum 10™ software. Multiple FTIR spectra were taken for each material (monomer and polymers) and maleimide signals (695 and 828 $cm^{-1}$) were evaluated with an error of $\pm$ 2 % based upon other signals in the spectra that did not change during the course of polymerization. Soxhlet extraction experiments with acetonitrile were completed in duplicate for each polymer network over a 24-hour period. The data indicated gel fractions to be > 98% for each network. The solvent was then removed under vacuum from the soluble portion and the residue was analyzed using FTIR as described above. Glass transition temperature ($T_g$) values were found using a TA Instruments Q200 Differential Scanning Calorimeter. $T_g$ values were determined from the inflection point of the second heating event at a heating rate of 2 °C/min from 90 to 120 °C on 5-8 mg of sample. No change in $T_g$ from the first to second heating was observed for any sample indicting that no annealing occurred as a result of the experimental conditions. A total of six replicate experiments were conducted for each PIL-CAN

formulation), resulting in an error of ± 1.4 °C. Thermal stability is defined by $T_{d5\%}$, the temperature at which 5% mass loss was observed. $T_{d5\%}$ values were determined using a TA Instruments Q500 on 4-6 mg samples under nitrogen from 30-800 °C at a ramp rate of 10 °C/min. Triplicate experiments were run on each PIL-CAN formulation, resulting in an error of ± 2 °C.

Oscillatory rheology was conducted using a TA Instruments DHR-2 rheometer with a standard 20-mm parallel plate setup. Strain sweeps were initially conducted at 100 °C from 0.1 to 10 rad/s to verify that the materials were in the linear viscoelastic regime (LVR). A strain of 0.5% was chosen based upon these LVR experiments. Storage ($G'$) and loss ($G''$) moduli were monitored in triplicate for each polymer as a function of frequency (0.05 to 100 rad/sec) at various temperatures over a range of temperatures (90-120 °C). Reported $T_{crossover}$ values have an error ± 3 °C. Dynamic mechanical analysis (DMA) was utilized to determine elastic storage modulus ($E'$) and tan delta curves, in film tension mode with a single frequency of 1 Hz at a heating rate of 5 °C/min from -50 to 125 °C. Tensile testing was also conducted using the TA Instruments Q800 DMA. Polymer samples were cut into rectangular strips and secured with the film clamps. The extension was increased at a rate of 20 mm/min at 25 $^0$C until each sample broke. Evaluation of each PIL-CAN formulation was completed in triplicate, and reported stress and strain at break measurements were reported as an average.

A TA Instruments DHR-2 Discovery Hybrid Rheometer with dielectric accessory and Keysight Technologies E4980AL/120 LCR meter was utilized to determine anhydrous conductivities of the PIL-CANs. A sample (thickness 250-300 μm) was placed between the two 25 mm stainless steel, parallel plate electrodes of the dielectric accessory and the environmental chamber, under an atmosphere of dry nitrogen and cooled with liquid nitrogen, was closed. Dielectric permittivity and conductivity were measured isothermally with an ac amplitude of ± 0.01 V in 10 °C steps over a frequency range of 20.0-$10^6$ Hz while being kept at a constant axial force of 5.0 ± 0.2 N. Each sample was allowed to soak for 45 minutes at each temperature prior to any measurement. DC-conductivity ($\sigma_{DC}$) was determined from the plateau value observed in the spectral dependence of the conductivity function ($\sigma' = \omega\varepsilon''\varepsilon_o$ where $\omega$ is the frequency, $\varepsilon''$ is the dielectric loss and $\varepsilon_o$ is the vacuum permittivity).

**Rehealing Studies.**

Determination of stress/strain recovery was completed as follows. Films were cut width wise with a razor blade to simulate a break point/fracture. The two cut ends were then overlapped by ~2 mm and were finger pressed together for several seconds. The materials were then placed in a convection oven at the desired temperature (105 $^{0}$C) and removed at various time intervals for tensile testing. A 200 g Teflon$^{TM}$ block was placed gently on top of the samples to ensure that good contact was being made throughout the experiment. Stress and strain are reported for each sample at break point. Here, a polymer is defined as "self-healing" if a new break point was observed away from the original re-seal point with at least 70% recovery of the stress and strain at the break of the original (uncut) polymer. Tensile (stress/strain) testing was conducted as previous described.

For stress relaxation tests, a rectangular specimen was placed into the grips of a TA Instruments Q800 DMA in tensile mode. Extension of the material was increased at a rate of 1 mm/s until a strain of 20% had been achieved. This strain was maintained for 4 hours while the stress was monitored.

For creep testing, a rectangular specimen was placed into the grips of a TA Instruments Q800 DMA in tensile mode. Extension of the material was increased at a rate of 0.5 mm/s until a stress equal to 50% of the stress of break of the original sample had been achieved. The stress was maintained for 4 hours while strain was monitored. The stress was then released to observe creep recovery.

**Conductivity Recovery:**

This process was developed as a modification of procedure published by Evans et al.[4] Two parallel planar electrodes were prepared by adhering 7-mm-wide copper tape onto a thin sheet of PTFE affixed to the surface of a glass slide; the gap between electrodes was 3 mm (an image of the electrode and sample configuration is provided in Figure S28). A 15-mm × 25-mm × 0.3-mm rectangular piece of re-healable ionic polymer was placed on top of the electrodes and heated to 110 °C in an Espec BTL-433 benchtop oven. Unless otherwise noted, a thin PTFE spacer and 500 g mass was kept on top of the polymer sample to provide pressure throughout the experiment.

While equilibrating at the desired temperature of 110 °C, chronoamperometric cycling between ±2V versus open circuit potential was initiated, with current recorded for 5 s at each potential per cycle. Continuous cycling of potential between ±2V and concomitant measurement

of current continued throughout the remainder of the experiment; however, at the end of every 30 minutes of cycling, there was a 2-3 minute "rest" period during which the open circuit potential was (re)measured and the current at 0 V was briefly monitored. Once the sample temperature/measured current had stabilized, the 500 g mass was removed from the top of the sample, and the sample region between the electrodes was cut with a clean razor blade. The razor blade was held in the cut for 1 minute, then removed. Another minute was allowed to pass before the 500 g weight was replaced on top of the sample. Current was monitored until it had re-stabilized, due to re-healing, after the cut. A summary of this experimental procedure in the form of a flow chart is shown in Figure S29. All electrochemical measurements were performed with a Metrohm Autolab PGSTAT302N potentiostat. After the current/conductivity recovery experiment was complete, the sample was allowed to cool, and then was inspected under a microscope. An image of the polymer after cut and reheal is shown in Figure S30.

**Synthetic Procedures.**

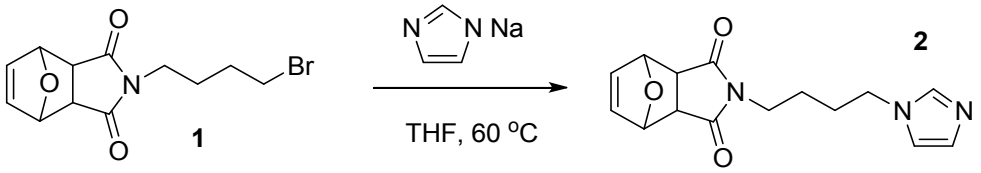


**Preparation of FUR-MA-imidazole 2.** To a 250-mL round-bottomed flask was suspended sodium imidazole (2.00 g, 0.0222 mol) in anhydrous THF (30 mL) under argon. To this stirred suspension was added a solution of furan-protected *N*-(4-bromobutyl)maleimide **1** (6.34 g, 0.0211 mol) in anhydrous THF (70 mL) dropwise via an addition funnel over a 30 minute period. After the addition was completed, the resulting mixture was warmed to 60 °C whereupon it was held for 36 hours. The mixture was then filtered and the solvent removed to give a yellow oil. The oil was partitioned between ethyl acetate and water. The organic phase was removed, washed with brine, dried over $Na_2SO_4$/$MgSO_4$, filtered and solvent removed to provide 5.04 g (79 %) of a light yellow oil. $^1$H NMR (400 MHz, DMSO-$d_6$, TMS): δ 7.53 (1 H, s, Im-$H^2$), 7.07 (1 H, s, Im-$H^4$), 6.82 (1 H, s, Im-$H^5$), 6.51 (2 H, s, -C*H*=C*H*-), 5.08 (2 H, s, C*H*-O), 3.47 (2 H, t, $J$ = 7.2 Hz, -C$H_2$-Im), 3.30 (2 H, t, $J$ = 7.3 Hz, -C$H_2$-NC(O)), 2.88 (2 H, s, C*H*-C(O)N), 1.71 (2 H, m, -C$H_2$-CH$_2$-Im), 1.55 (2 H, m, -C$H_2$-CH$_2$-NC(O)). $^{13}$C NMR (100 MHz, DMSO-$d_6$, TMS): δ 176.27, 136.98, 136.12,

128.08, 118.91, 80.09, 46.82, 45.00, 36.87, 27.41, 23.59. Elem. Anal.: Calc. for $C_{15}H_{17}N_3O_3$: C, 62.7; H, 6.0; N, 14.6 %; Found: C, 62.4; H, 6.1; N, 14.8 %.

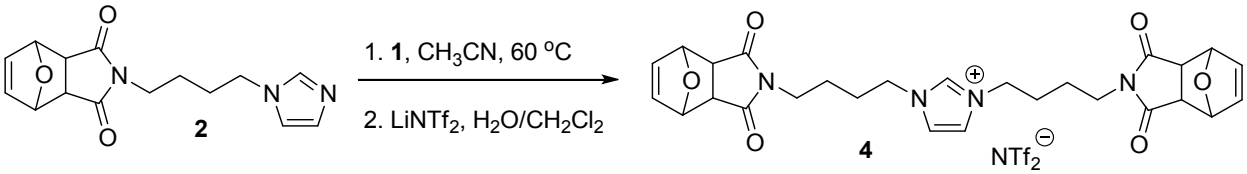


**Preparation of FUR-MA-IM $NTf_2$ 4.** To a 50-mL round-bottomed flask was dissolved FUR-MA-imidazole **2** (1.00 g, 3.48 mmol) in acetonitrile (20 mL). Furan-protected *N*-(4-bromobutyl)maleimide **1** (1.10 g, 3.66 mmol) was then added and the resulting solution was warmed to 60 °C where it was held for 24 hours. The solvent was then removed under reduced pressure, affording a light pink oil. Ethyl acetate (50 mL) was added and a light pink precipitate formed which was further isolated, washed with additional ethyl acetate (3 x 50 mL) and dried under vacuum overnight. Yield of the final, light pink solid was found to be 1.72 g (84 %). $^1$H NMR (400 MHz, DMSO-$d_6$, TMS): δ 9.27 (1 H, s, Im-$H^2$), 7.82 (1 H, s, Im-$H^4$), 7.74 (1 H, s, Im-$H^5$), 6.55 (4 H, s, -C*H*=C*H*-), 5.11 (4 H, s, C*H*-O), 4.15 (4 H, m,-C$H_2$-Im), 3.35 (4 H, m, -C$H_2$-NC(O)), 2.92 (4 H, s, C*H*-C(O)N), 1.66-1.83 (4 H, m, -C$H_2$-CH$_2$-Im), 1.40 (2 H, m, -C$H_2$-NC(O)), 1.24 (2 H, m, -C$H_2$-CH$_2$-NC(O)). $^{13}$C NMR (100 MHz, DMSO-$d_6$, TMS): δ 176.65, 136.47, 136.02, 122.41, 80.37, 48.20, 47.16, 37.07, 26.48, 23.67. Elem. Anal.: Calc. for $C_{27}H_{31}BrN_4O_6$: C, 55.2; H, 5.3; N, 9.5 %; Found: C, 55.3; H, 5.2; N, 9.4 %. To a 100-mL round-bottomed flask was dissolved FUR-MA-IM Br (1.05 g, 1.79 mmol) in DI water (15 mL). To this stirred solution was added a solution of lithium bis(trifluoromethanesulfonyl)imide (0.52 g, 1.82 mmol) in DI water (10 mL). An immediate reaction occurred resulting in the formation of a gummy precipitate. Dichloromethane (25 mL) was added to dissolve the precipitate and the resulting mixture was stirred at RT overnight. The organic phase was then removed, washed with DI water (3 x 15 mL) and dried under reduced pressure, affording 1.32 g (93 %) of a light pink oil. $^1$H NMR (400 MHz, DMSO-$d_6$, TMS): δ 9.11 (1 H, s, Im-$H^2$), 7.73 (2 H, s, Im-$H^{4,5}$), 6.55 (4 H, s, -C*H*=C*H*-), 5.11 (4 H, s, C*H*-O), 4.16 (4 H, m,-C$H_2$-Im), 3.35 (4 H, m, -C$H_2$-NC(O)), 2.91 (4 H, s, C*H*-C(O)N), 2.65-2.76 (4 H, m, -C$H_2$-CH$_2$-Im), 1.31-1.48 (4 H, m, -C$H_2$-CH$_2$-NC(O)). $^{13}$C NMR (100 MHz, DMSO-$d_6$, TMS): δ 176.63, 136.46, 136.05, 122.45, 119.47 (q, $J$ = 321 Hz, -*C*F$_3$), 80.38, 48.15, 47.14,

37.08, 26.47, 23.67. Elem. Anal.: Calc. for $C_{29}H_{31}F_6N_5O_{10}S_2$: C, 44.2; H, 4.0; N, 8.9 %; Found: C, 44.3; H, 3.9; N, 9.1 %.

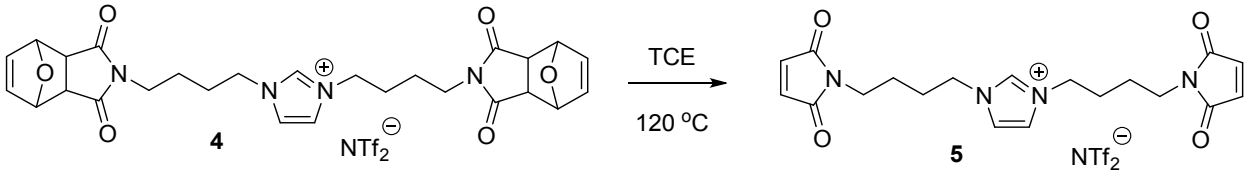


**Preparation of MA-IM NTf$_2$ 5.** To a 100-mL round-bottomed flask, equipped with a magnetic stir bar and short path distillation head (cold water cooled) and collection flask, was dissolved FUR-MA-IM NTf$_2$ **4** (1.03 g, 1.30 mmol) in 1,1,2,2-tetrachloroethane (20 mL). The stirred solution was warmed to 120 °C where it was held for 24 hours. The solvent was then removed under reduced pressure to afford a light yellow oil (0.81 g, 96 %). $^1$H NMR (400 MHz, DMSO-$d_6$, TMS): δ 9.12 (1 H, s, Im-$H^2$), 7.76 (2 H, s, Im-$H^{4,5}$), 7.00 (4 H, s, -C*H*=C*H*-), 4.15 (4 H, m,-C$H_2$-Im), 3.40 (4 H, m, -C$H_2$-NC(O)), 1.73 (4 H, m, -C$H_2$-CH$_2$-Im), 1.45 (2 H, m, -C$H_2$-CH$_2$-NC(O)). $^{13}$C NMR (100 MHz, DMSO-$d_6$, TMS): δ 171.13, 136.25, 134.53, 122.48, 119.50 (q, $J$ = 325 Hz, -*C*F$_3$), 48.37, 36.33, 26.70, 24.73. Elem. Anal.: Calc. for $C_{21}H_{23}F_6N_5O_8S_2$: C, 38.7; H, 3.6; N, 10.8 %; Found: C, 38.5; H, 3.4; N, 10.6 %.

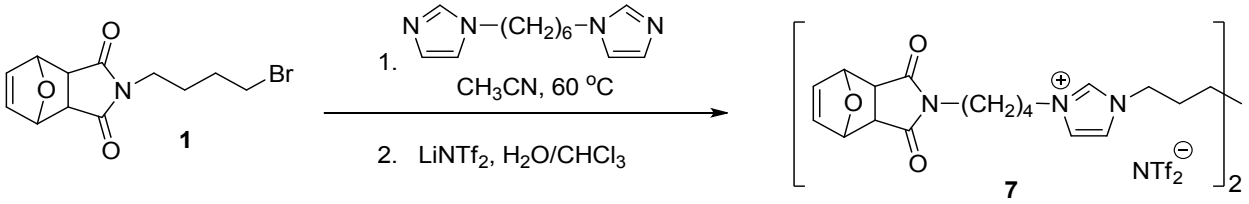


**Preparation of FUR-MA-IM2 NTf$_2$ 7.** To a 250-mL round-bottomed flask equipped with a magnetic stir bar was dissolved furan-protected *N*-(4-bromobutyl)maleimide **1** (7.80 g, 25.0 mmol) and 1,1′-(1,6-hexanediyl)bisimidazole (2.70 g, 12.4 mmol) in acetonitrile (100 mL). The solution was stirred at 60 °C for 48 hours, then the residuals were removed under reduced pressure to afford a viscous red oil. Vigorous washing with tetrahydrofuran (3 x 100 mL), followed by removal of residuals under high vacuum, resulted in a light pink solid (8.47 g, 84 %). $^1$H NMR (400 MHz, DMSO-$d_6$, TMS): δ 9.28 (2 H, s, Im-$H^2$), 7.82 (2 H, s, Im-$H^4$), 7.76 (2 H, s, Im-$H^5$), 6.53 (4 H, s,

-C*H*=C*H*-), 5.09 (4 H, s, C*H*-O), 4.17 (8 H, m,-C$H_2$-Im), 3.36 (4 H, m, -C$H_2$-NC(O)), 2.91 (4 H, s, C*H*-C(O)N), 1.65-1.85 (8 H, m, -C$H_2$-C$H_2$-Im), 1.40 (4 H, m, -C$H_2$-C$H_2$-NC(O)), 1.24 (4 H, m, -C$H_2$-C$H_2$-C$H_2$-Im). $^{13}$C NMR (100 MHz, DMSO-$d_6$, TMS): δ 176.65, 136.46, 136.04, 122.54, 122.35, 80.37, 48.69, 48.18, 47.16, 37.10, 29.01, 26.54, 24.84, 23.69. Elem. Anal.: Calc. for $C_{36}H_{36}Br_2N_6O_2$: C, 52.8; H, 5.7; N, 10.3 %; Found: C, 53.1; H, 5.8; N, 10.1 %. To a 500-mL round-bottomed flask equipped with a magnetic stir bar was dissolved FUR-MA-IM2 Br salt (6.50 g, 7.94 mmol) in DI water (80 mL). To this stirred solution was added a solution of lithium bis(trifluoromethylsulfonyl)imide (4.79 g, 16.7 mmol) in DI water (40 mL). A mixture immediately formed and dichloromethane (100 mL) was added to aid in dissolution and mixing. The mixture stirred at room temperature for 24 hours. The organic phase was then separated, washed with DI water (3 x 75 mL), and volatiles removed under reduced pressure to afford a viscous light pink oil (9.27 g, 96 %). $^1$H NMR (400 MHz, DMSO-$d_6$, TMS): δ 9.09 (2 H, s, Im-*H*$^2$), 7.73 (2 H, s, Im-*H*$^4$), 7.70 (2 H, s, Im-*H*$^5$), 6.51 (4 H, s, -C*H*=C*H*-), 5.08 (4 H, s, C*H*-O), 4.13 (8 H, m,-C$H_2$-Im), 3.34 (4 H, m, -C$H_2$-NC(O)), 2.88 (4 H, s, C*H*-C(O)N), 1.65-1.80 (8 H, m, -C$H_2$-C$H_2$-Im), 1.39 (4 H, m, -C$H_2$-C$H_2$-NC(O)), 1.22 (4 H, m, -C$H_2$-C$H_2$-C$H_2$-Im). $^{13}$C NMR (100 MHz, DMSO-$d_6$, TMS): δ 176.63, 136.46, 135.98, 122.53, 122.38, 119.75 (q, $J$ = 323 Hz, -*C*F$_3$), 80.39, 48.79, 48.23, 37.07, 30.67, 29.05, 26.53, 24.94, 23.69. Elem. Anal.: Calc. for $C_{40}H_{43}F_{12}N_8O_{14}S_4$: C, 39.4; H, 3.8; N, 9.2 %; Found: C, 39.2; H, 4.0; N, 9.3 %.

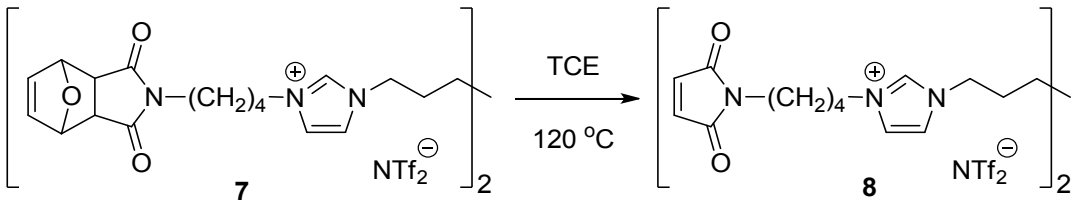

**7** **8**

**Preparation of MA-IM2 NTf$_2$ 8.** To a 250-mL round-bottomed flask, equipped with a magnetic stir bar and short path distillation head (cold water cooled) and collection flask, was dissolved FUR-MA-IM2 NTf$_2$ **7** (7.50 g, 6.15 mmol) in TCE (100 mL). The stirred solution was heated to 120 °C and held overnight. The solution was then cooled to 50 °C and high vacuum was applied to removed residual furan and TCE. The reaction yielded 6.52 g of a viscous pink oil (98 %). $^1$H NMR (400 MHz, DMSO-$d_6$, TMS): δ 9.12 (2 H, s, Im-*H*$^2$), 7.76 (4 H, s, Im-*H*$^{4,5}$), 7.04 (4 H, s, -C*H*=C*H*-), 4.17 (8 H, m,-C$H_2$-Im), 3.41 (4 H, m, -C$H_2$-NC(O)), 1.71-1.84 (8 H, m, -C$H_2$-C$H_2$-Im), 1.41 (4 H, m, -C$H_2$-C$H_2$-NC(O)), 1.25 (4 H, m, -C$H_2$-C$H_2$-C$H_2$-Im). $^{13}$C NMR (100 MHz, DMSO-

$d_6$, TMS): δ 171.14, 135.99, 134.55, 122.43, 119.46 (q, $J$ = 320 Hz, -$CF_3$), 48.76, 48.42, 36.36, 29.06, 26.71, 24.95, 24.75. Elem. Anal.: Calc. for $C_{32}H_{38}F_{12}N_8O_{12}S_4$: C, 35.5; H, 3.5; N, 10.4 %; Found: C, 35.4; H, 3.4; N, 10.6 %.

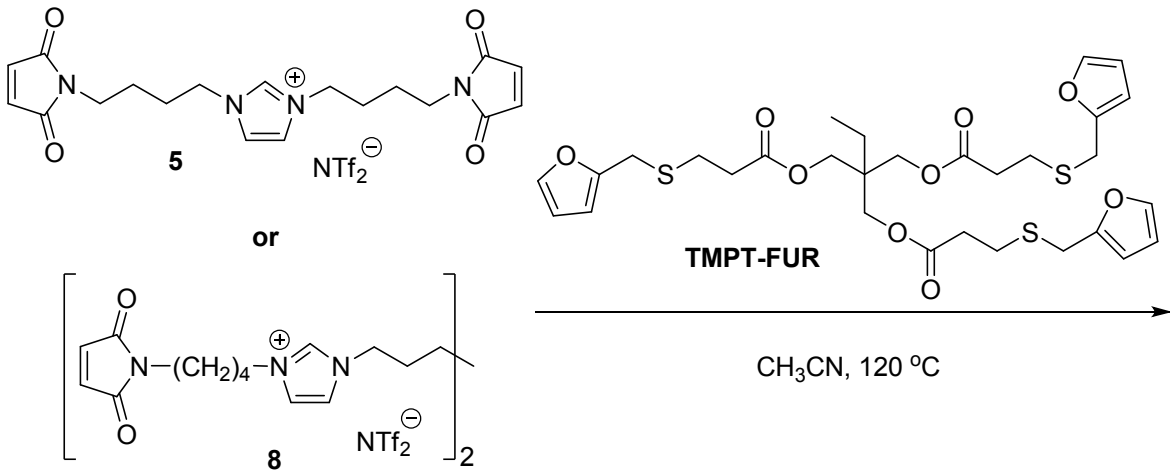


**Representative Example of Polymerization Procedure.** To an 8-mL vial was charged MA-IM2 $NTf_2$ **8** (0.40 g, 0.369 mmol) and TMPT-FUR (0.19 g, 0.246 mmol). Acetonitrile (0.6 g) was added and the resulting mixture was shaken until a solution resulted. The solution was transferred by pipet into an apparatus that consisted of a 40-mm × 30-mm rectangular Teflon™ mold with a glass bottom, held together with binder clips. The apparatus was placed into a convection oven at 120 °C until a solid film had formed (30-45 minutes). The apparatus was removed and allowed to cool to room temperature. The film was then placed into a vacuum oven (50 °C, < 0.1 mm Hg) for 24 hours to ensure residual solvent removal. Polymerization resulted in clear, flexible films with variable yellow/brown color with thicknesses between 250-300 μm. Polymers were found to revert completely to their liquid form upon reaching 125-130 °C.

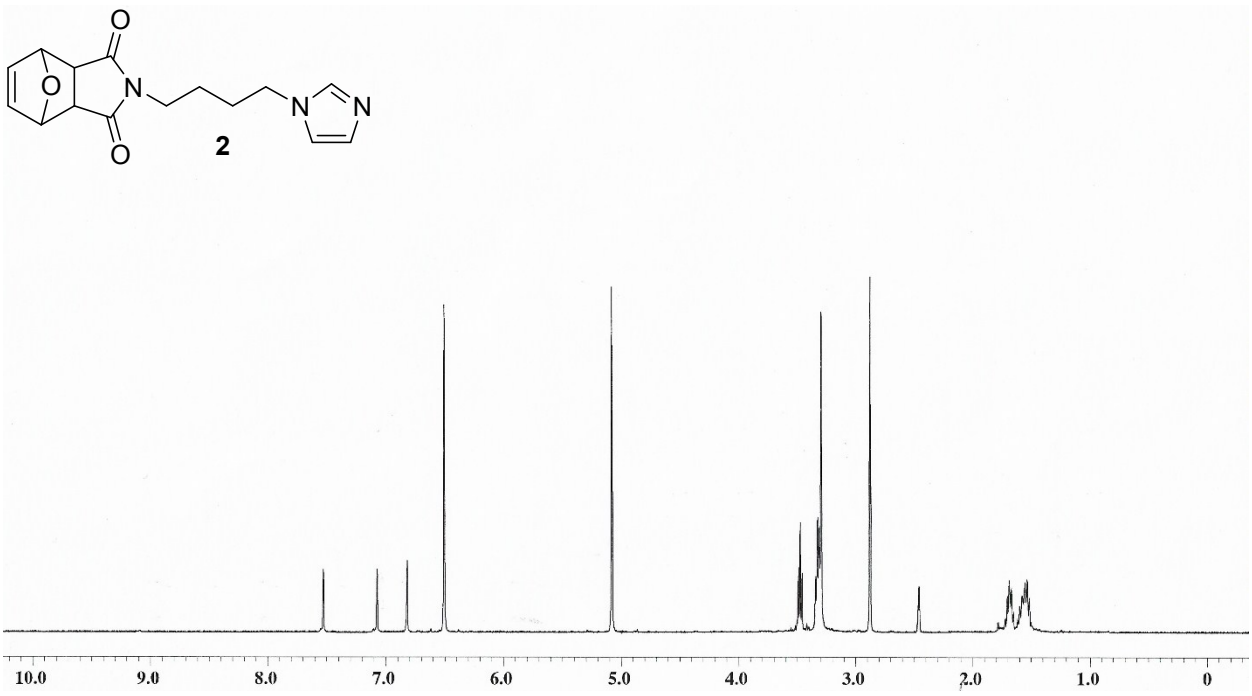


Figure S1: $^{1}$H NMR spectrum of **FUR-MA-imidazole 2** (DMSO-$d_6$)

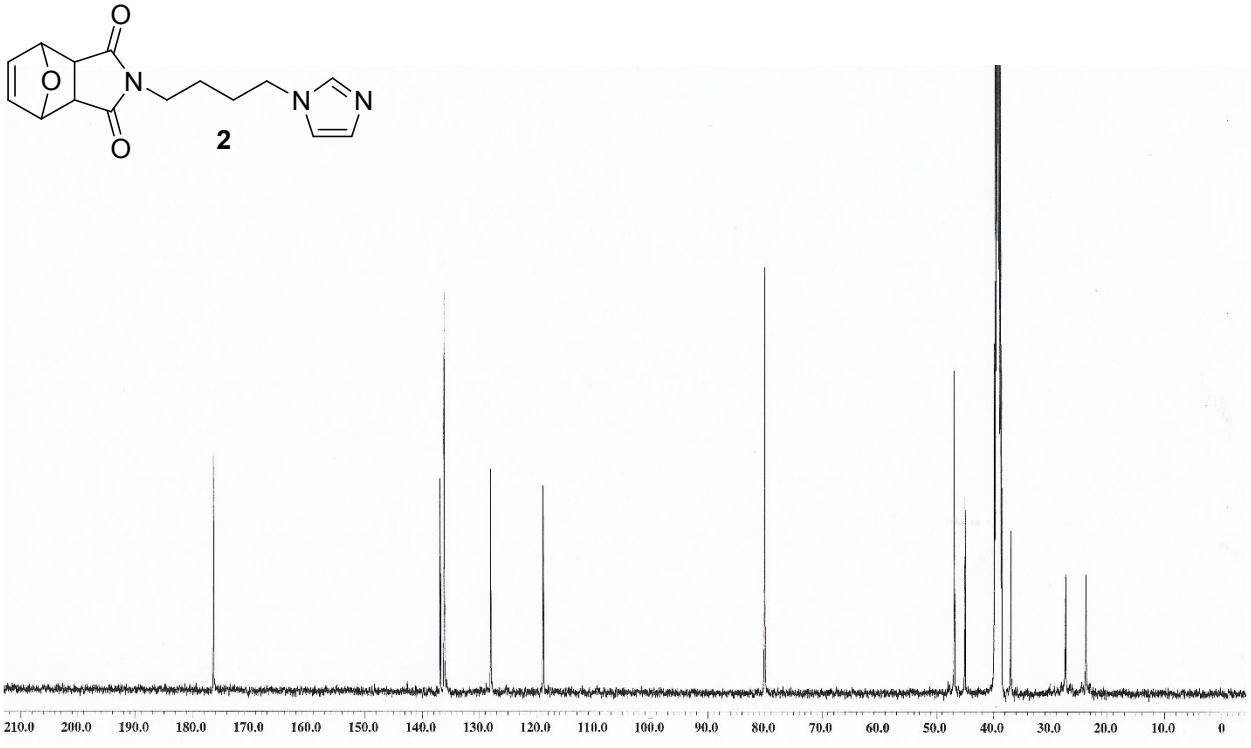


Figure S2: $^{13}$C NMR spectrum of **FUR-MA-imidazole 2** (DMSO-$d_6$)

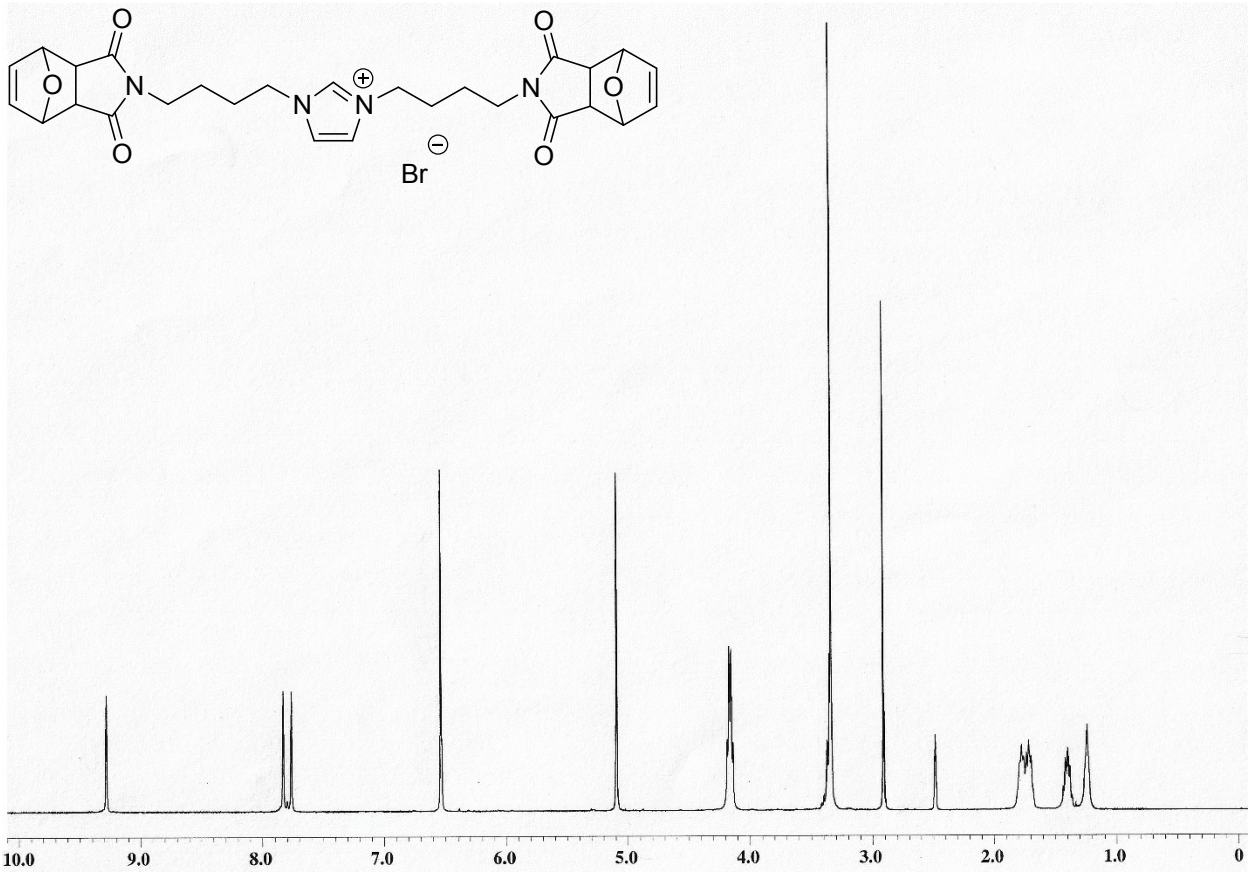


Figure S3: $^{1}$H NMR spectrum of **FUR-MA-IM Br** (DMSO-$d_6$)

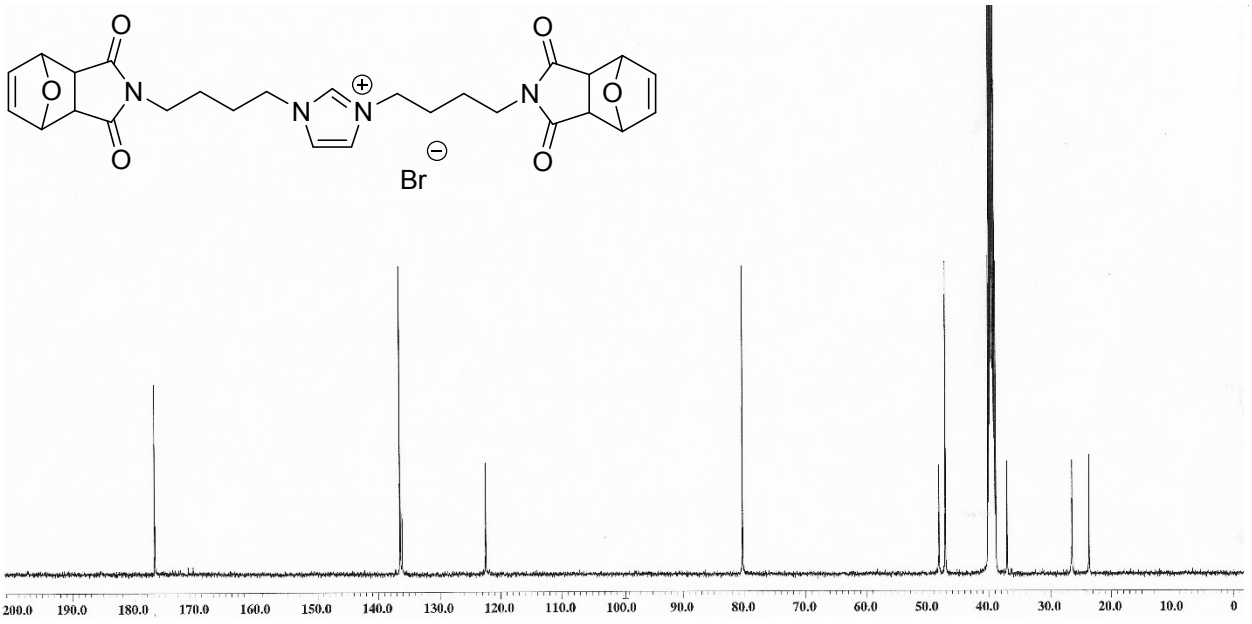


Figure S4: $^{13}$C NMR spectrum of **FUR-MA-IM Br** (DMSO-$d_6$)

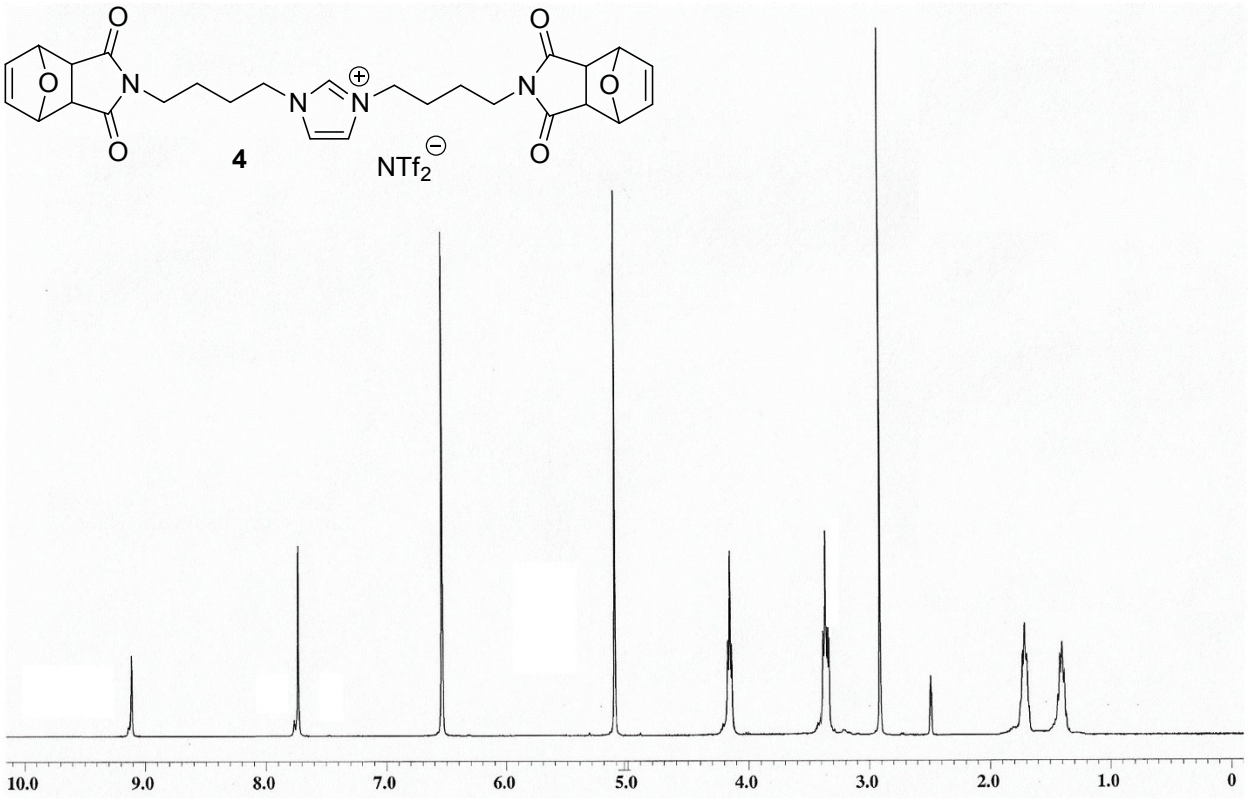


Figure S5: $^{1}$H NMR spectrum of **FUR-MA-IM NTf$_2$ 4** (DMSO-$d_6$)

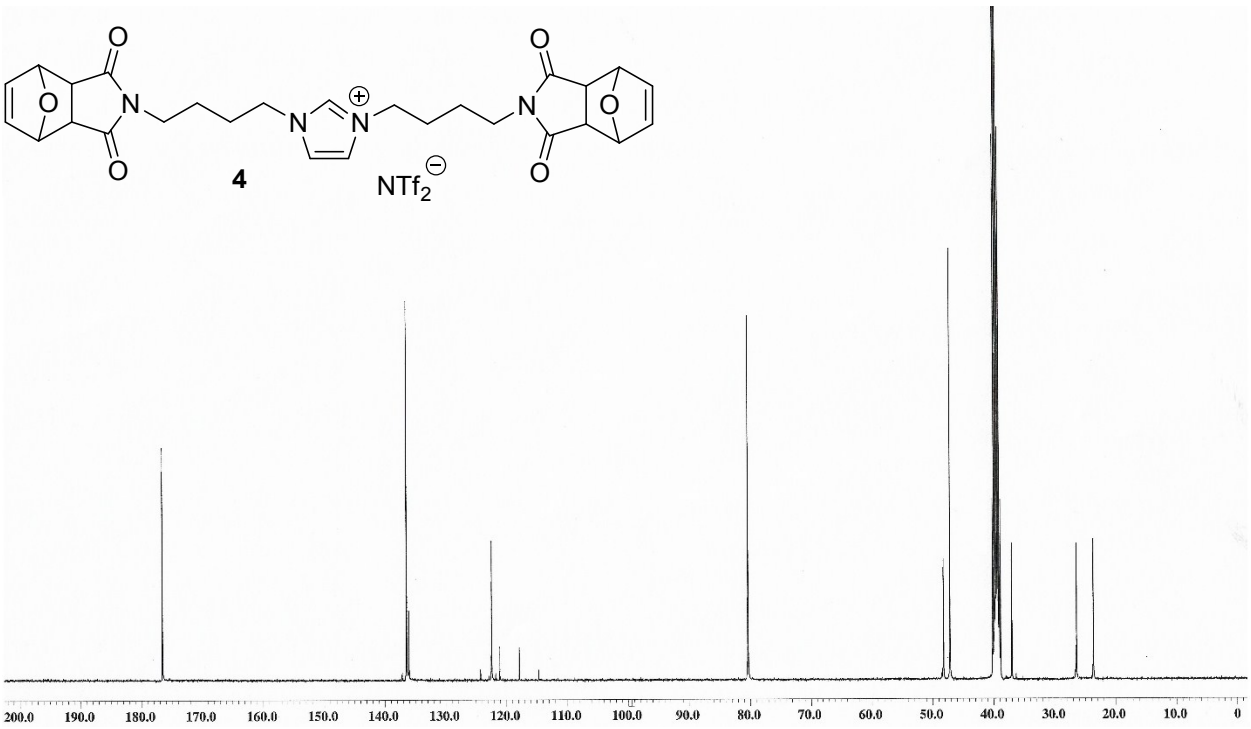


Figure S6: $^{13}$C NMR spectrum of **FUR-MA-IM NTf$_2$ 4** (DMSO-$d_6$)

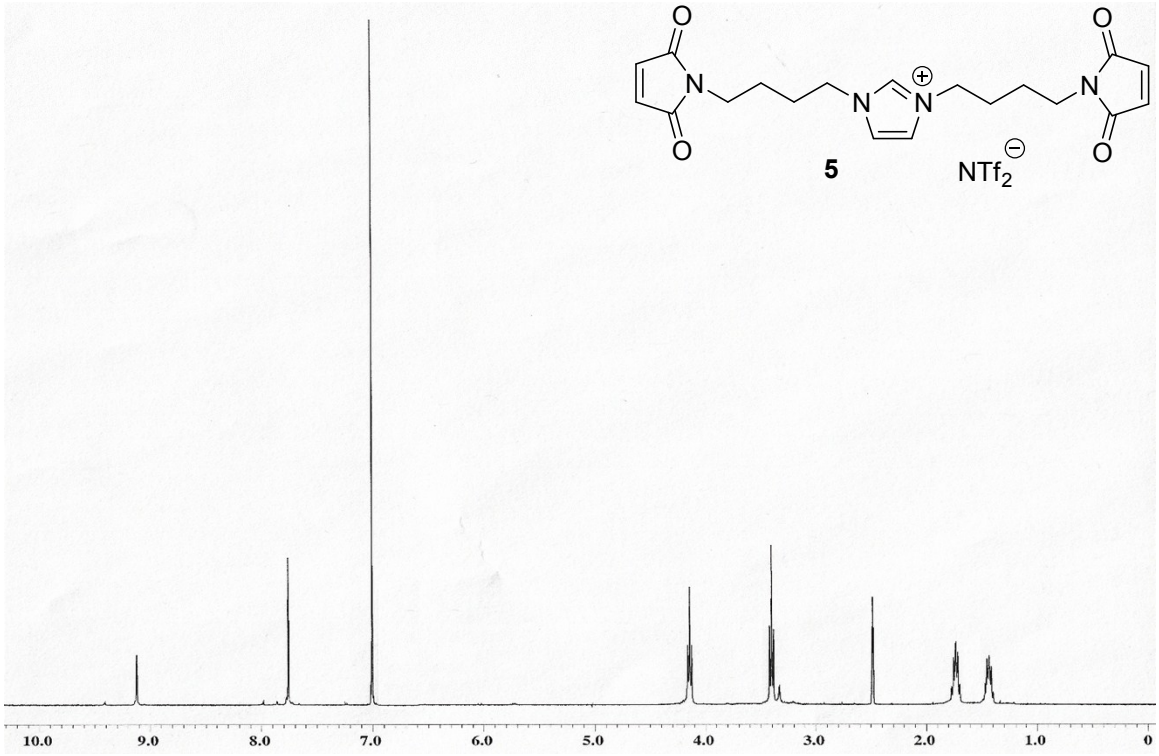


Figure S7: $^{1}$H NMR spectrum of **MA-IM NTf$_2$ 5** (DMSO-$d_6$)

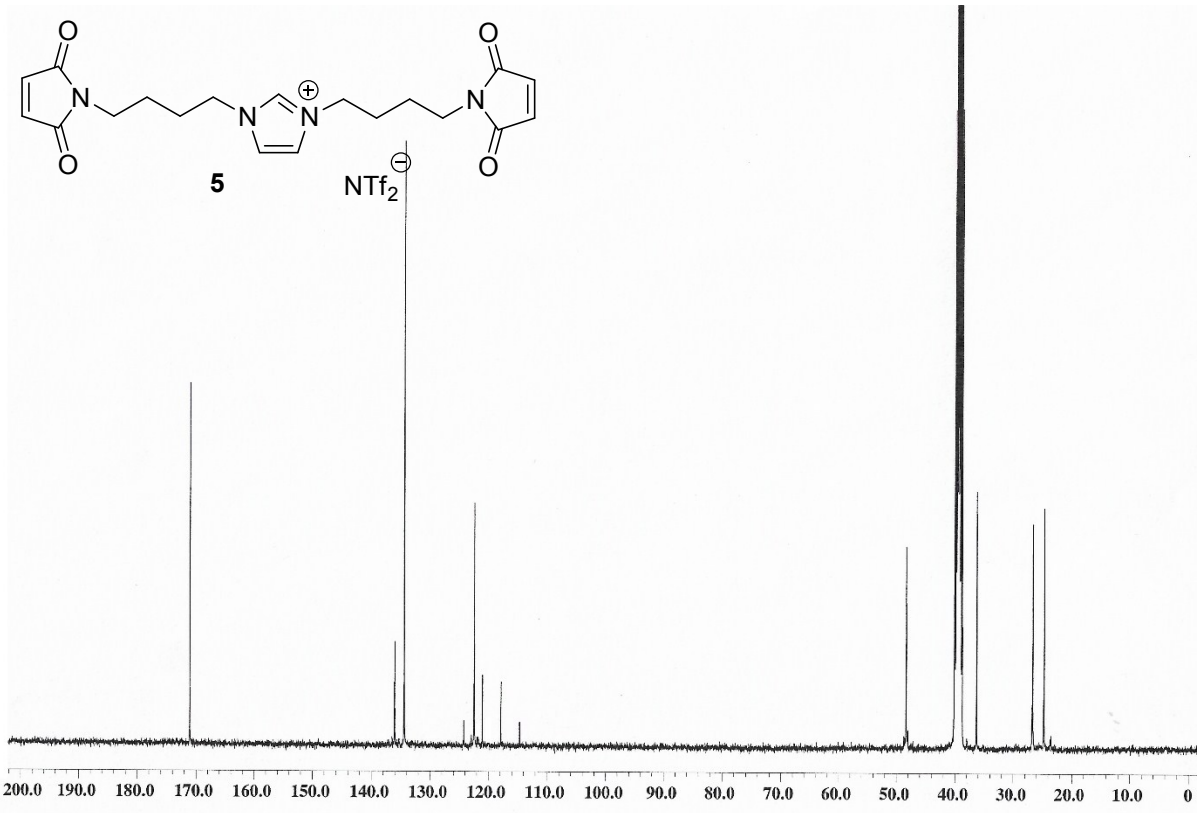


Figure S8: $^{13}$C NMR spectrum of **MA-IM NTf$_2$ 5** (DMSO-$d_6$)

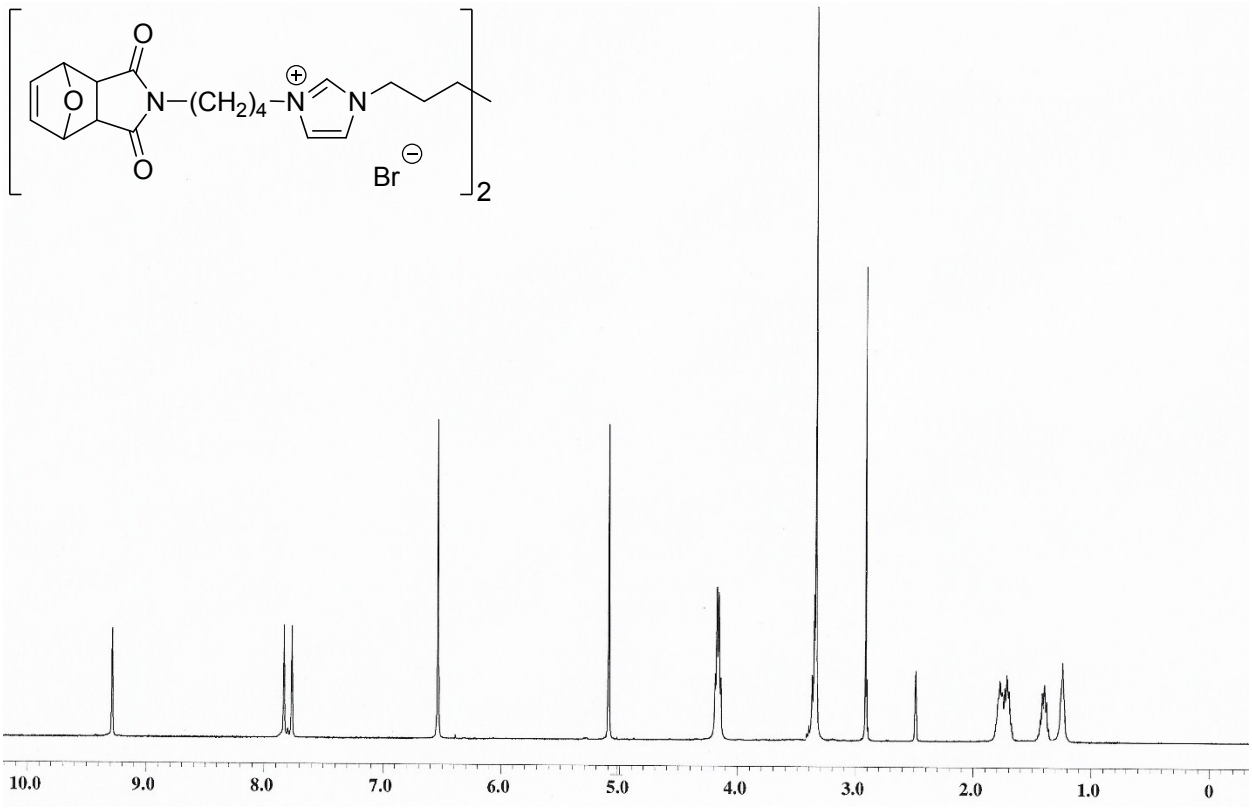


Figure S9: $^{1}$H NMR spectrum of **FUR-MA-IM2 Br** (DMSO-$d_6$)

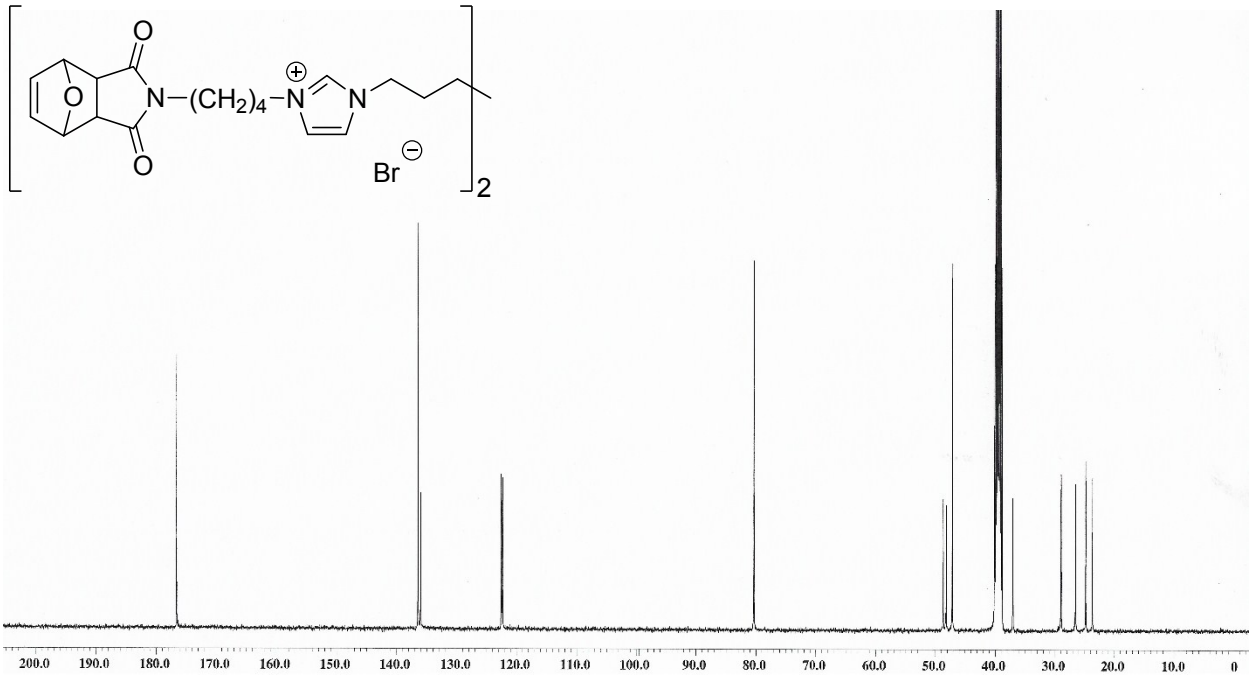


Figure S10: $^{13}$C NMR spectrum of **FUR-MA-IM2 Br** (DMSO-$d_6$)

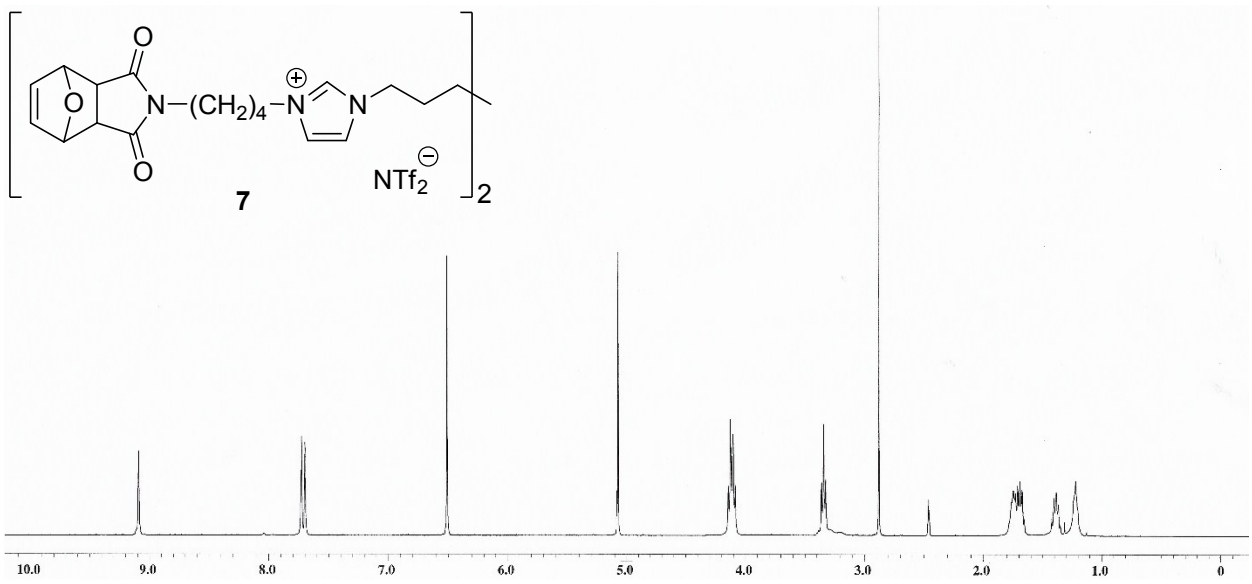


Figure S11: $^{1}$H NMR spectrum of **FUR-MA-IM2 NTf$_2$** (DMSO-$d_6$).

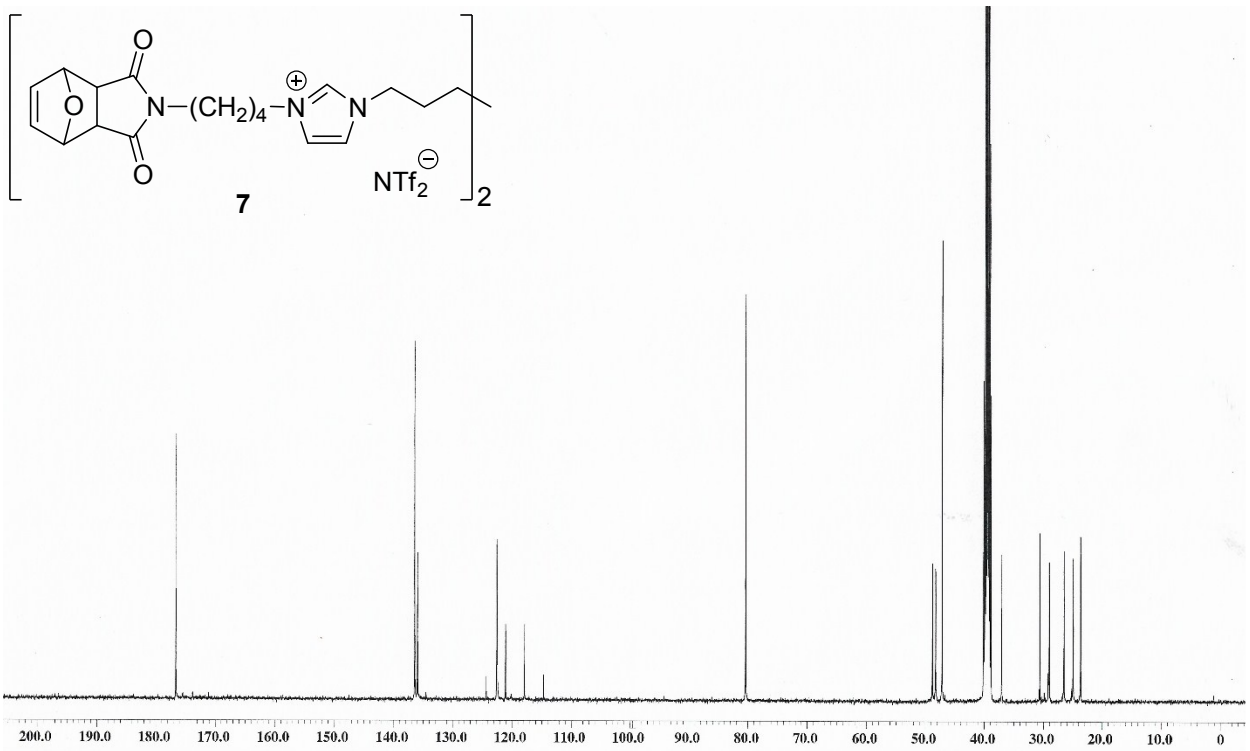


Figure S12: $^{13}$C NMR spectrum of **FUR-MA-IM2 NTf$_2$** (DMSO-$d_6$)

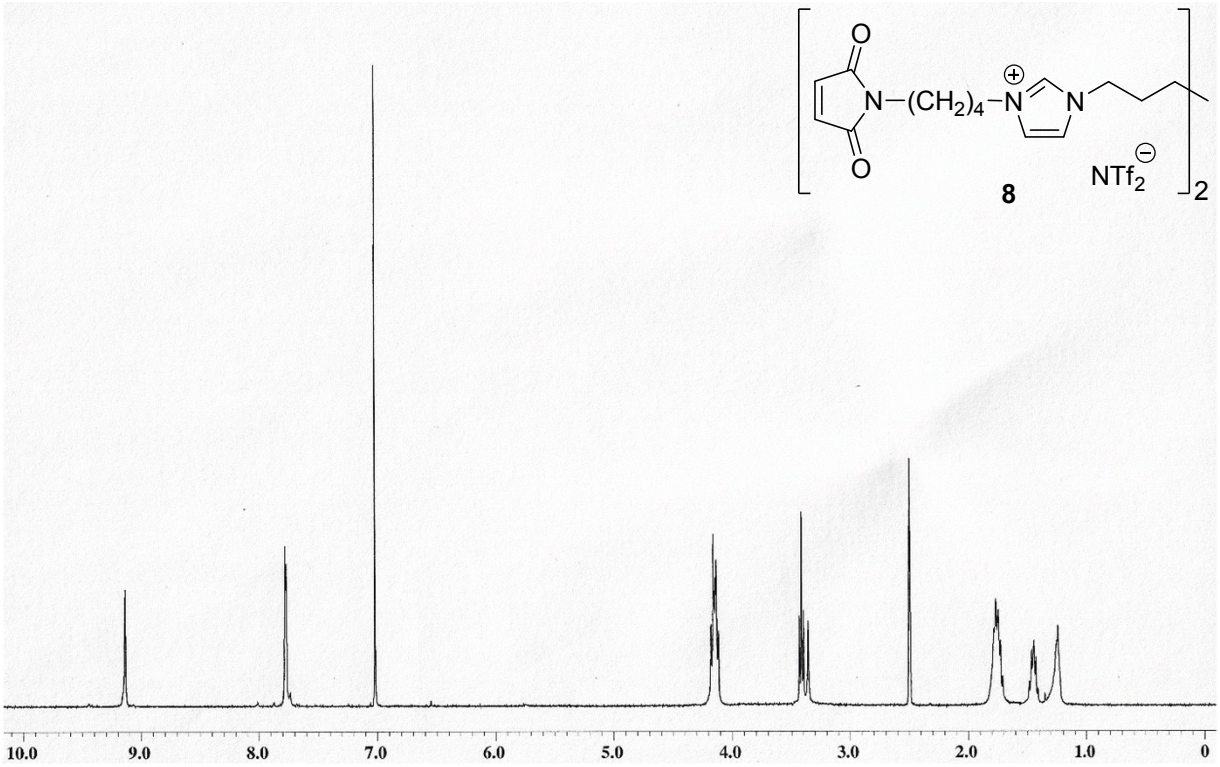


Figure S13: $^{1}$H NMR spectrum of **MA-IM2 NTf$_2$ 8** (DMSO-$d_6$)

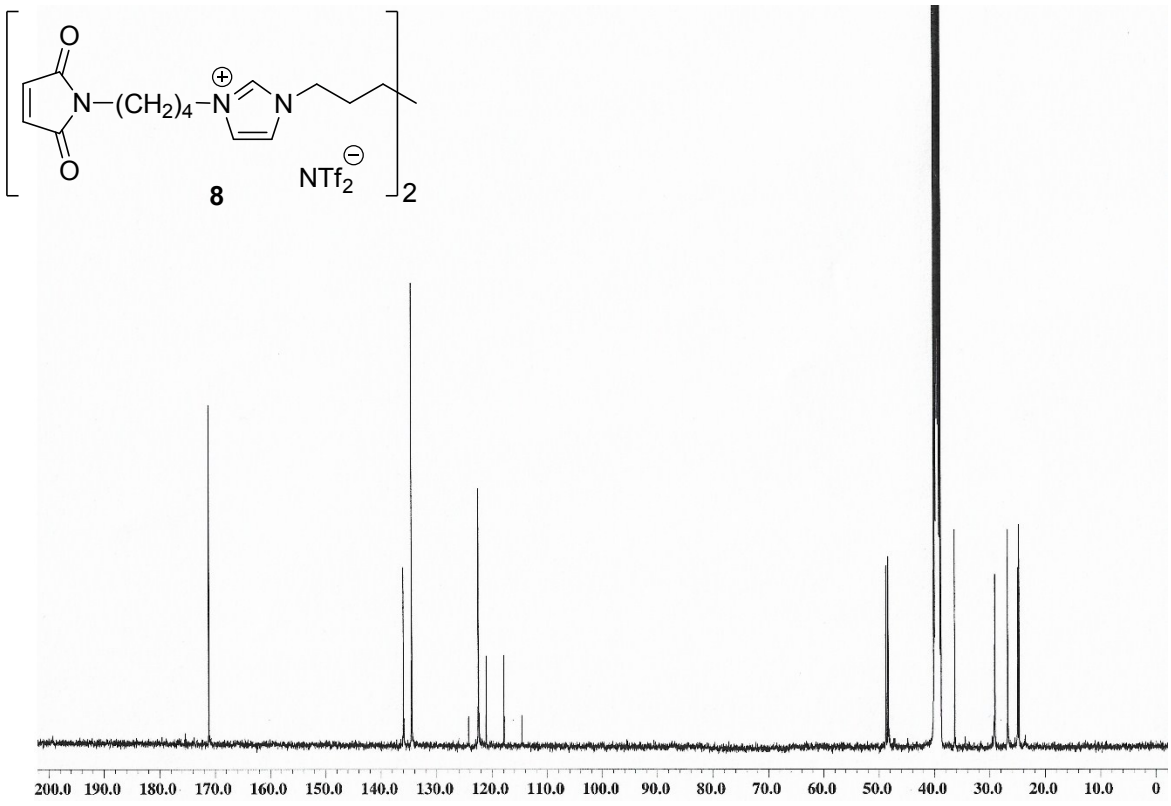


Figure S14: $^{13}$C NMR spectrum of **MA-IM2 NTf$_2$ 8** (DMSO-$d_6$)

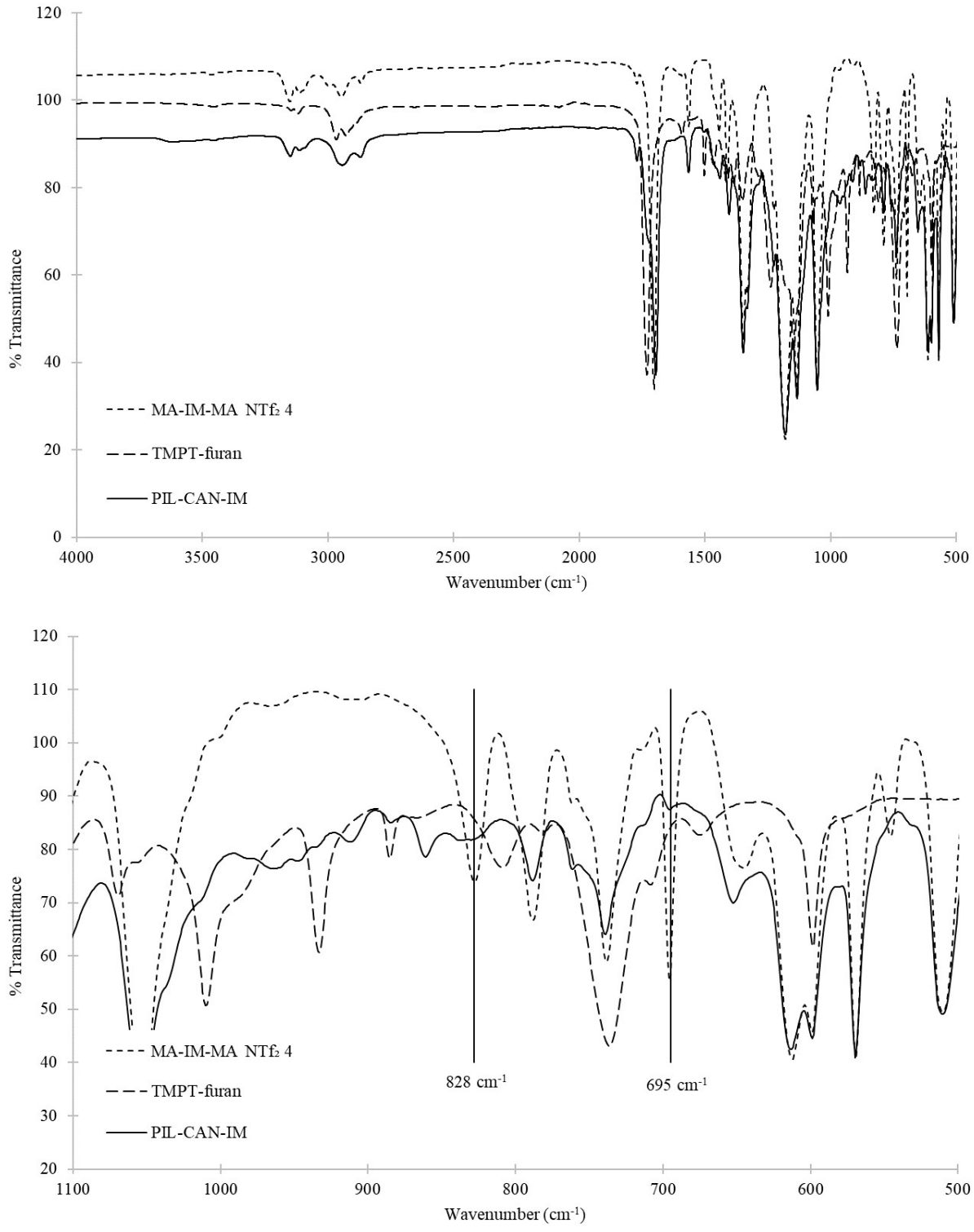


Figure S15: Overlay of FTIR spectra PIL-CAN-IM and precursor monomers. Top overlay is wide view and bottom overlay is expanded to see maleimide bands at 828 and 695 $cm^{-1}$.

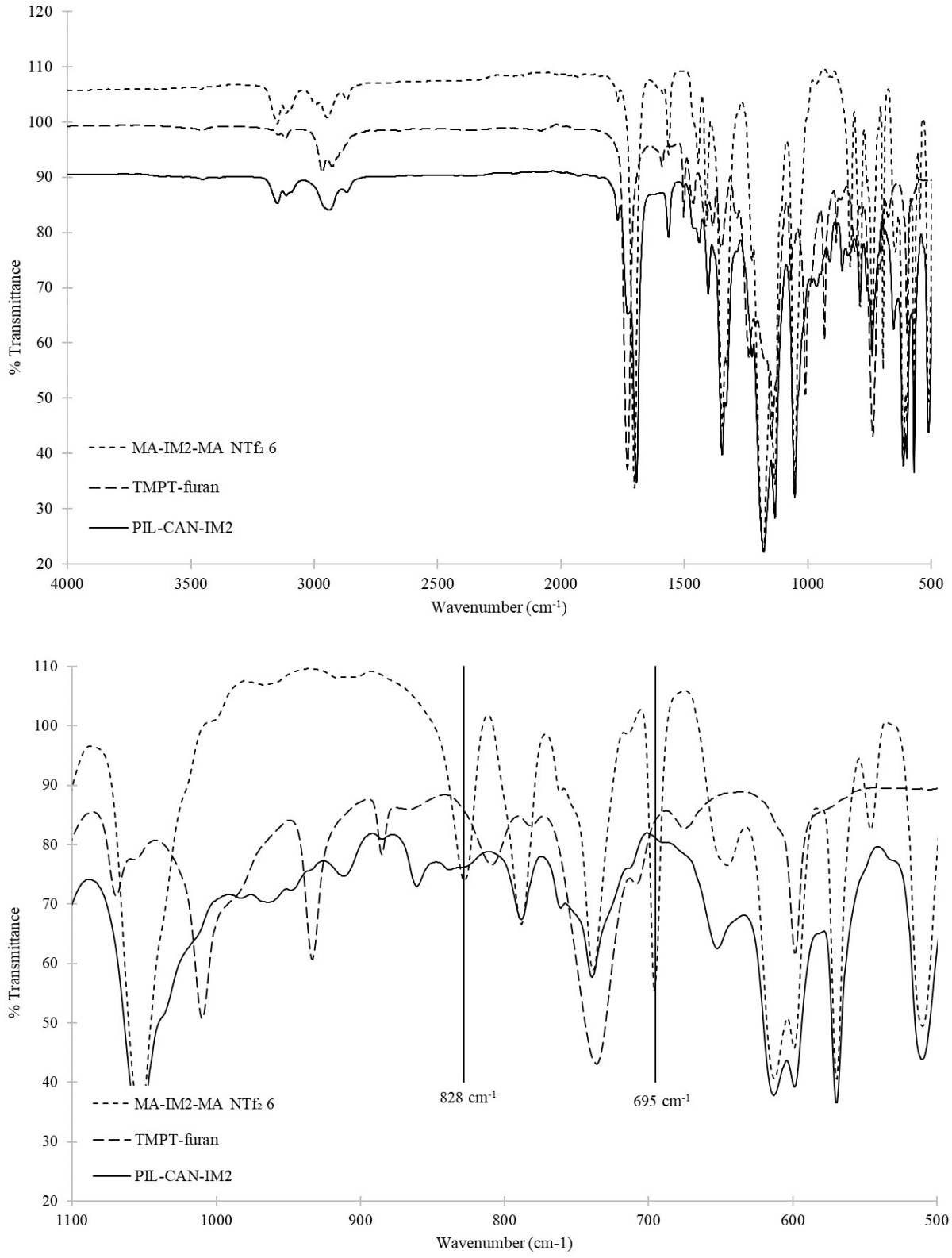


Figure S16: Overlay of FTIR spectra PIL-CAN-IM2 and precursor monomers. Top overlay is wide view and bottom overlay is expanded to see maleimide bands at 828 and 695 $cm^{-1}$.

Table S1: Summary of elemental analysis results for PIL-CANs.

| **PIL-CAN-IM** | **% C** | **% H** | **% N** |
|---|---|---|---|
| THEORY | 45.79 | 4.54 | 6.44 |
| SAMPLE A | 45.58 | 4.82 | 6.66 |
| SAMPLE B | 45.56 | 4.37 | 6.73 |
| SAMPLE C | 45.68 | 4.32 | 6.53 |
| SAMPLE D | 45.25 | 4.24 | 6.67 |
| SAMPLE E | 45.31 | 4.55 | 6.52 |
| AVG | 45.45 | 4.46 | 6.62 |
| **PIL-CAN-IM2** | **% C** | **% H** | **% N** |
| THEORY | 43.85 | 4.52 | 6.21 |
| SAMPLE A | 43.50 | 4.39 | 6.37 |
| SAMPLE B | 43.61 | 4.25 | 6.51 |
| SAMPLE C | 43.92 | 4.61 | 6.42 |
| SAMPLE D | 43.66 | 4.45 | 6.35 |
| SAMPLE E | 43.72 | 4.39 | 6.31 |
| AVG | 43.68 | 4.42 | 6.39 |

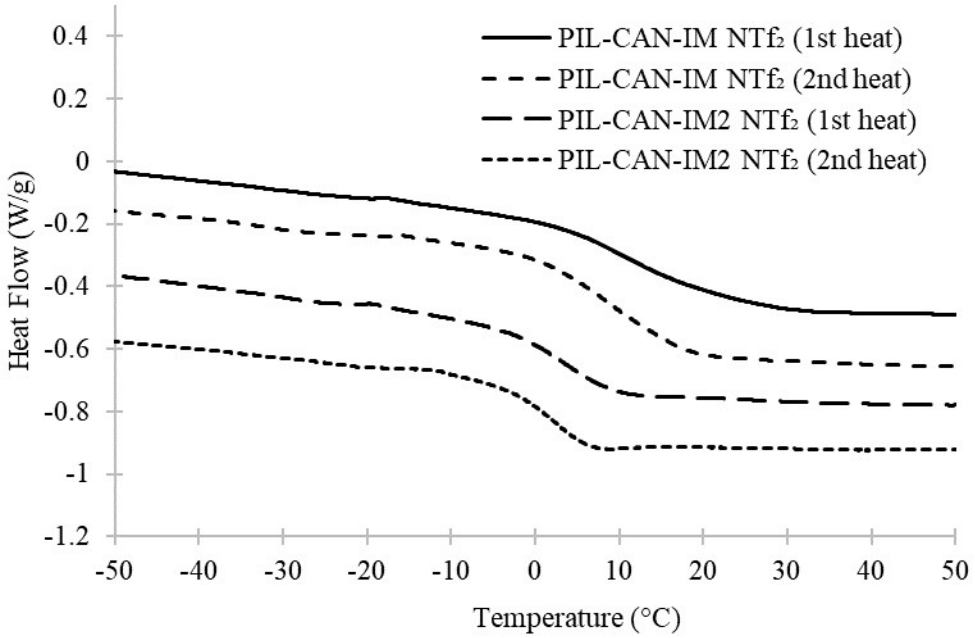


Figure S17: Overlay of DSC traces (1st and 2nd heating) for PIL-CAN-IM and PIL-CAN-IM2 networks.

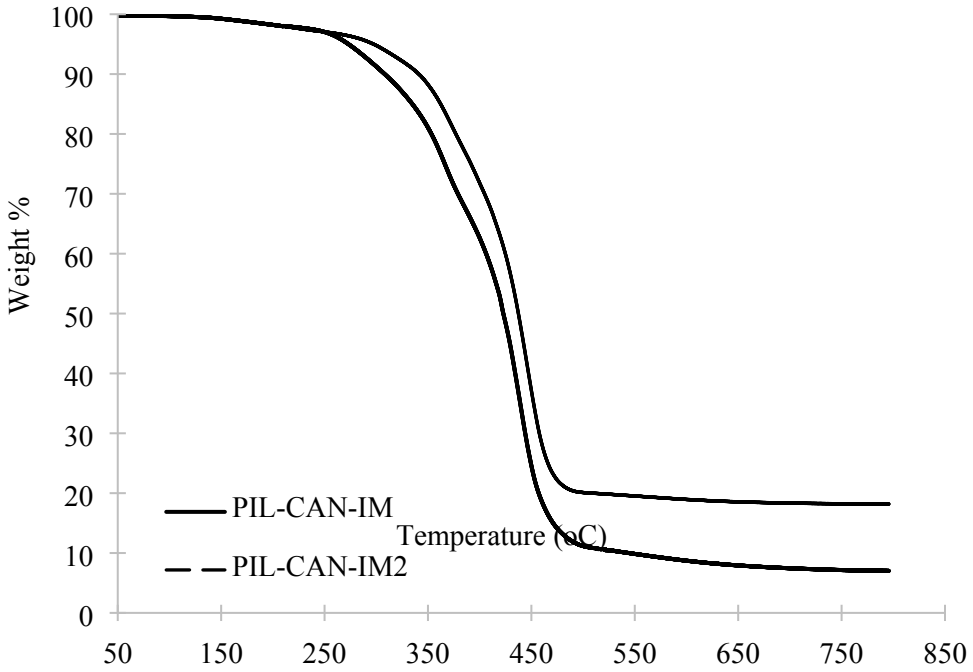


Figure S18: Overlay of TGA traces for PIL-CAN-IM and PIL-CAN-IM2 networks.

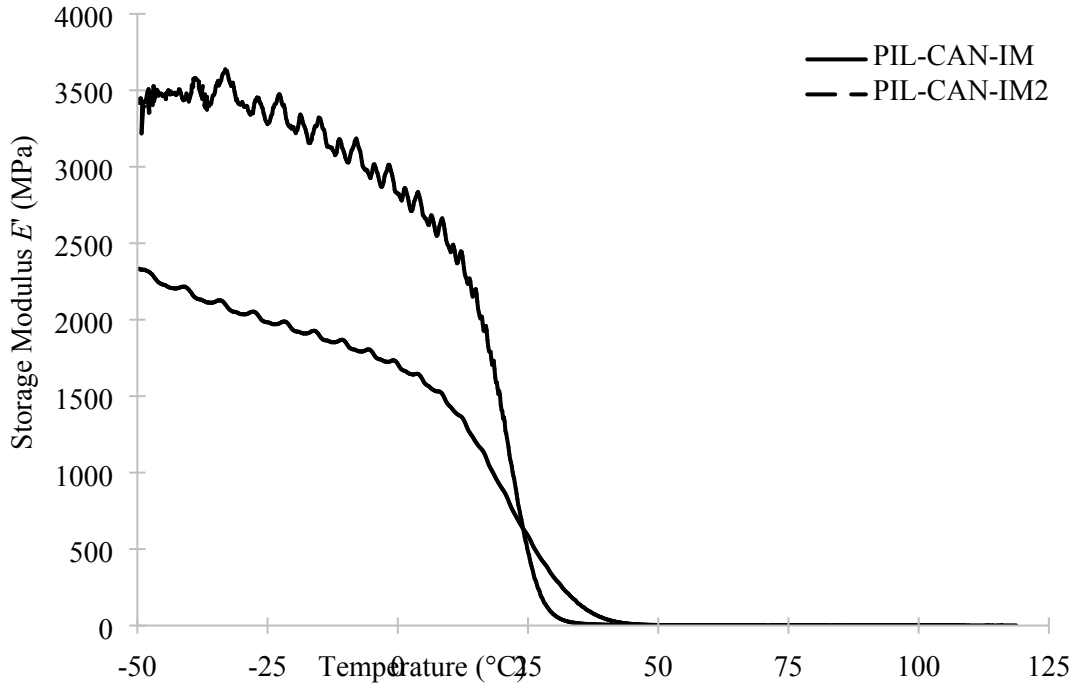


Figure S19: Overlay of DMA curves for PIL-CAN-IM and PIL-CAN-IM2 networks.

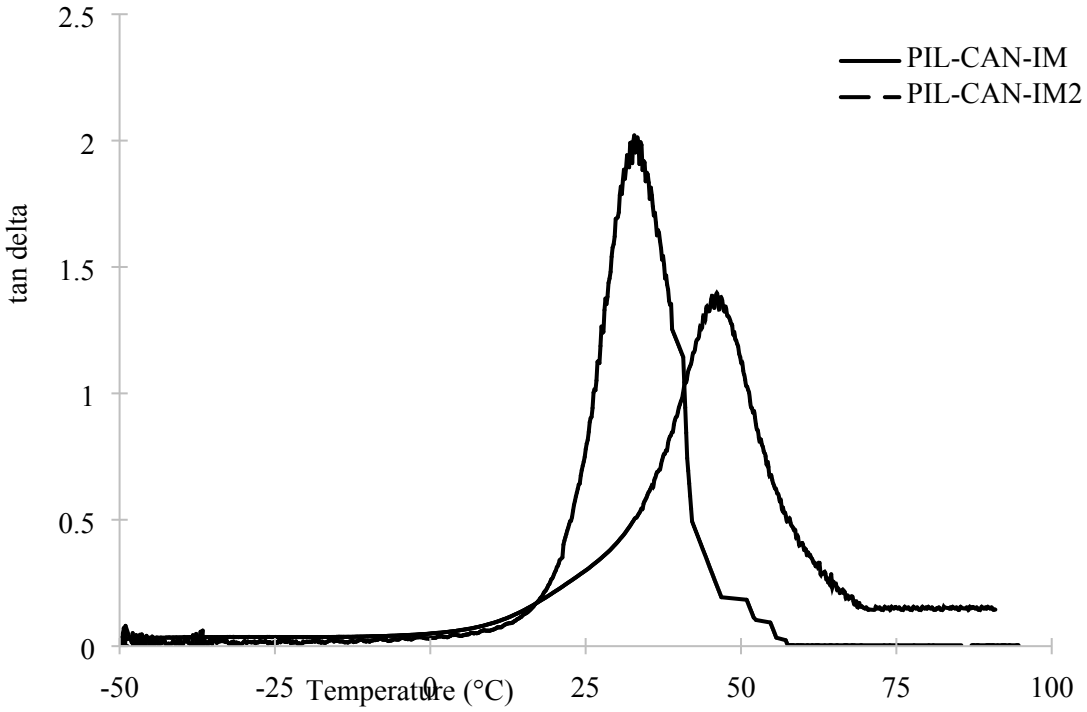


Figure S20: Overlay of tan δ curves for PIL-CAN-IM and PIL-CAN-IM2 networks.

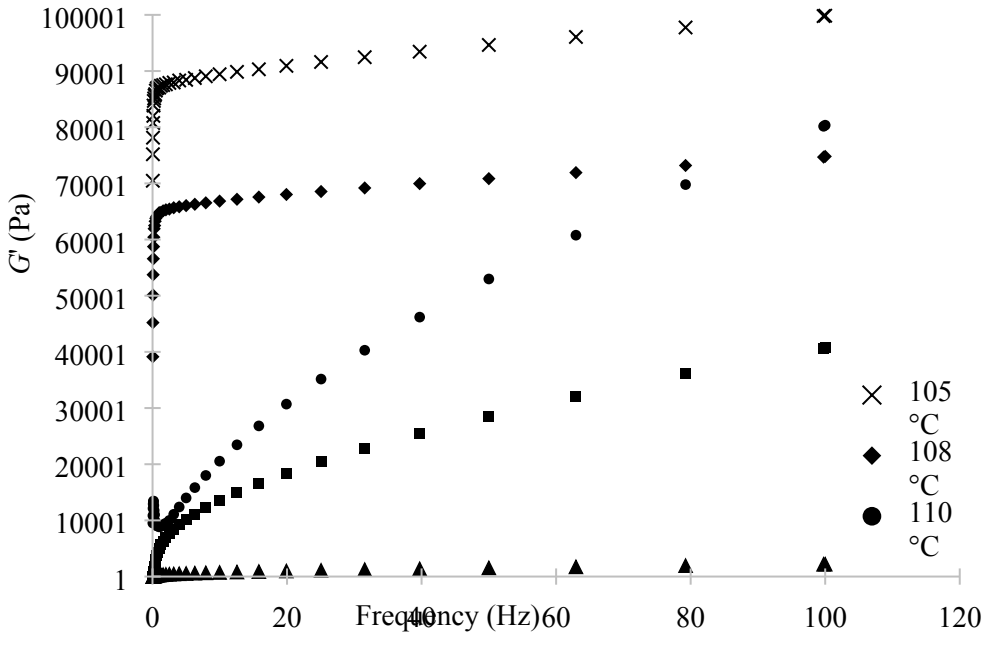


Figure S21: Elastic modulus versus frequency for the PIL-CAN-IM at various temperatures.

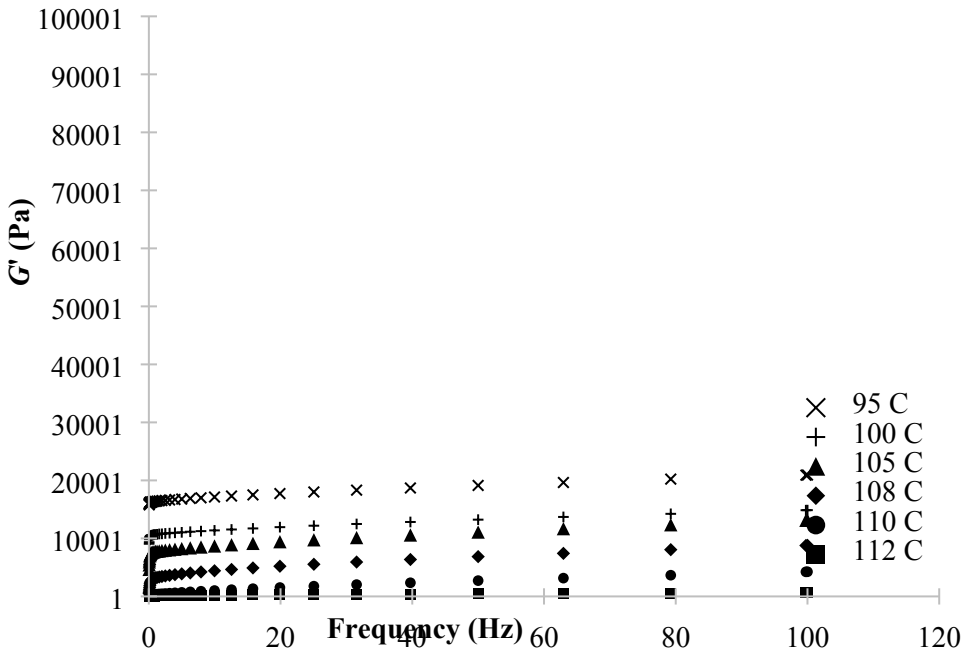


Figure 22: Elastic modulus versus frequency for the PIL-CAN-IM2 at various temperatures.

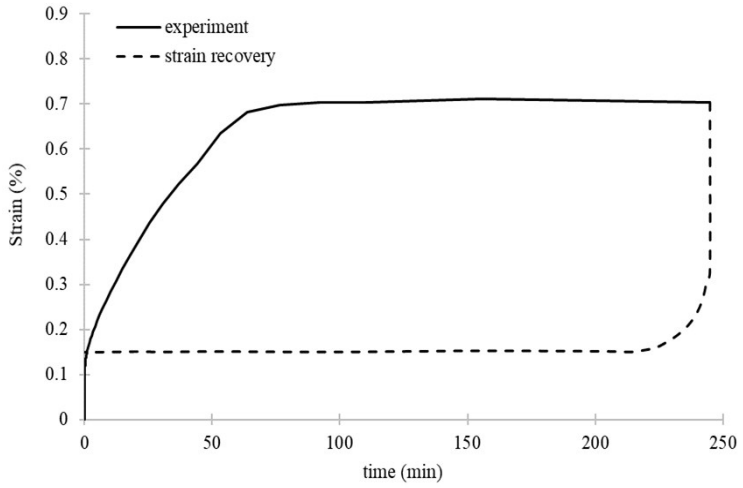


Figure S23: Creep recovery for PIL-CAN-IM.

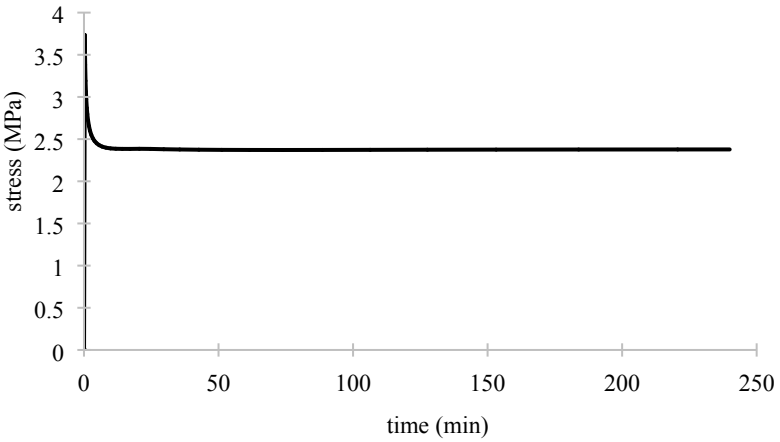


Figure S24: Stress relaxation study for PIL-CAN-IM.

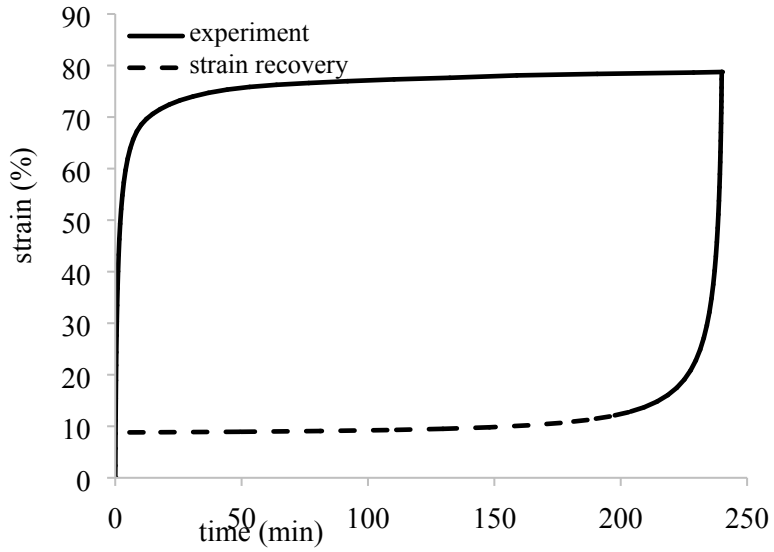


Figure S25: Creep recovery for PIL-CAN-IM2.

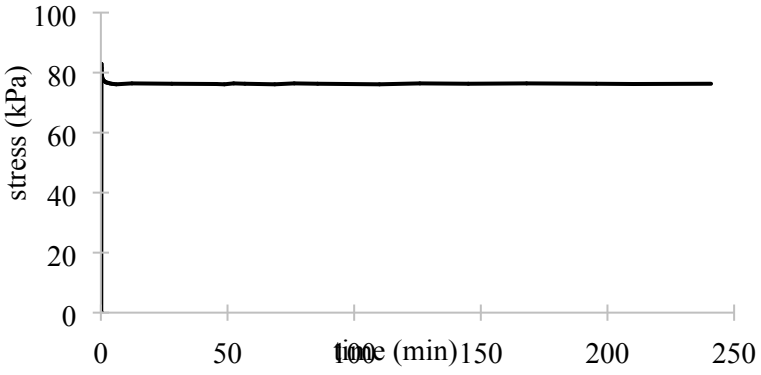


Figure S26: Stress relaxation study for PIL-CAN-IM2.

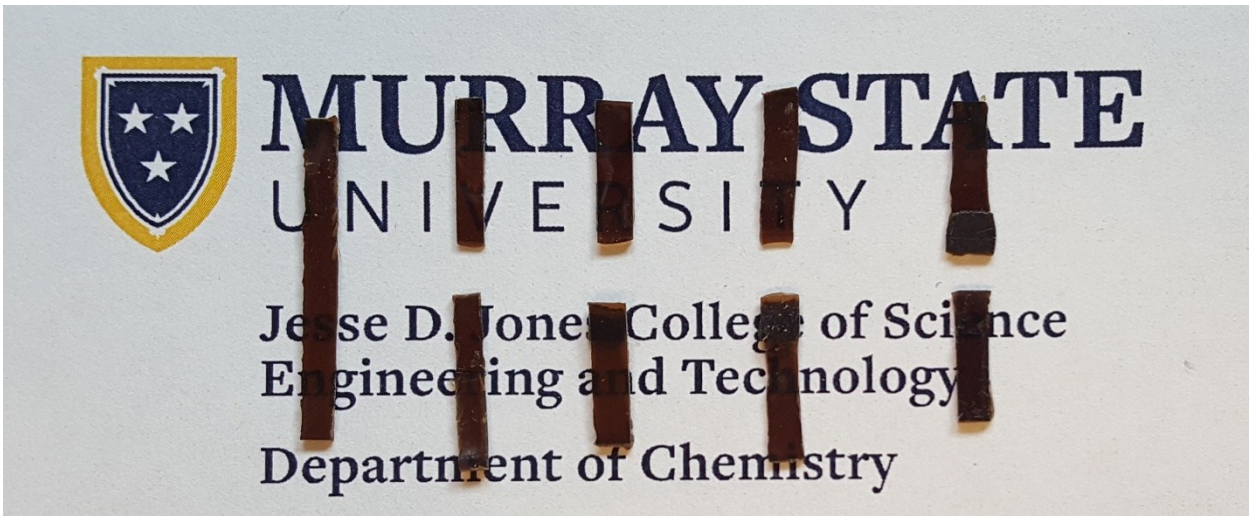


Figure S27A: Samples from a representative re-heal stress-strain trial for PIL-CAN-IM at 105 °C. From left-to-right: original sample, freshly cut sample, 1 hr re-heal sample, 2 hr re-heal sample, 4 hr re-heal sample.

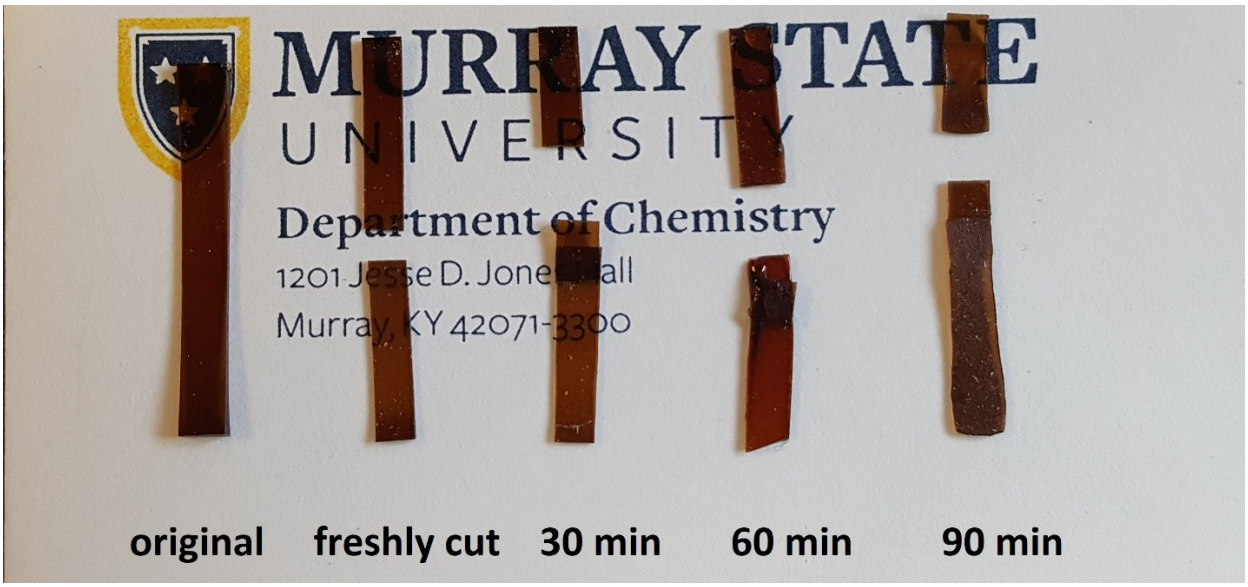


Figure S27B: Samples from a representative re-heal stress-strain trial for PIL-CAN-IM2 at 105 °C. From left-to-right: original sample, freshly cut sample, 30 min re-heal sample, 60 min re-heal sample, 90 min re-heal sample.

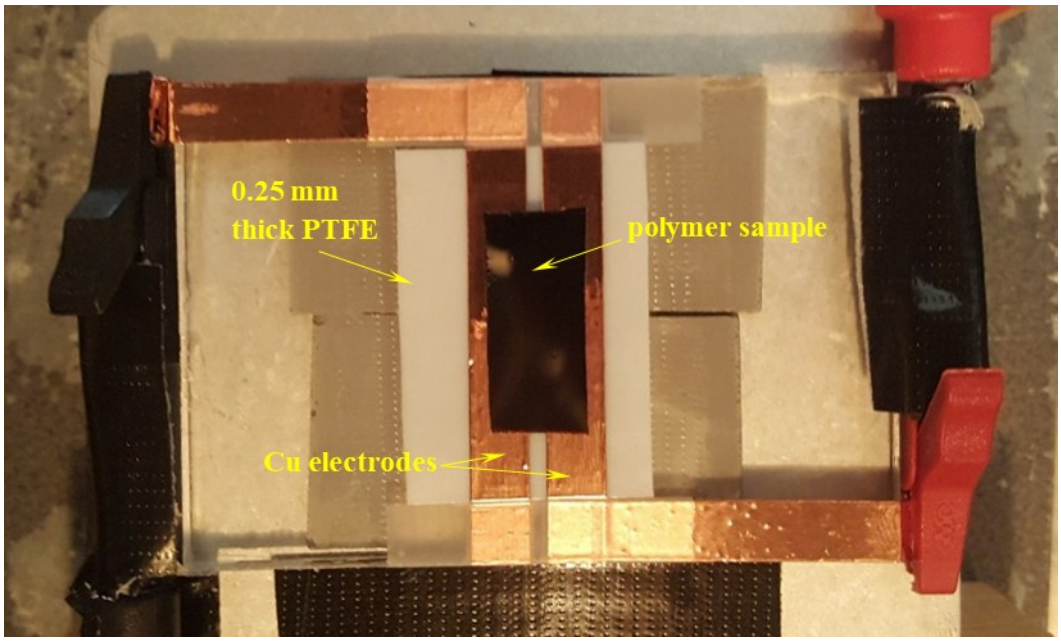


Figure S28: Electrode configuration (with sample) for recovery of conductivity experiments. Black and red alligator clips connect the individual Cu electrodes to a potentiostat.

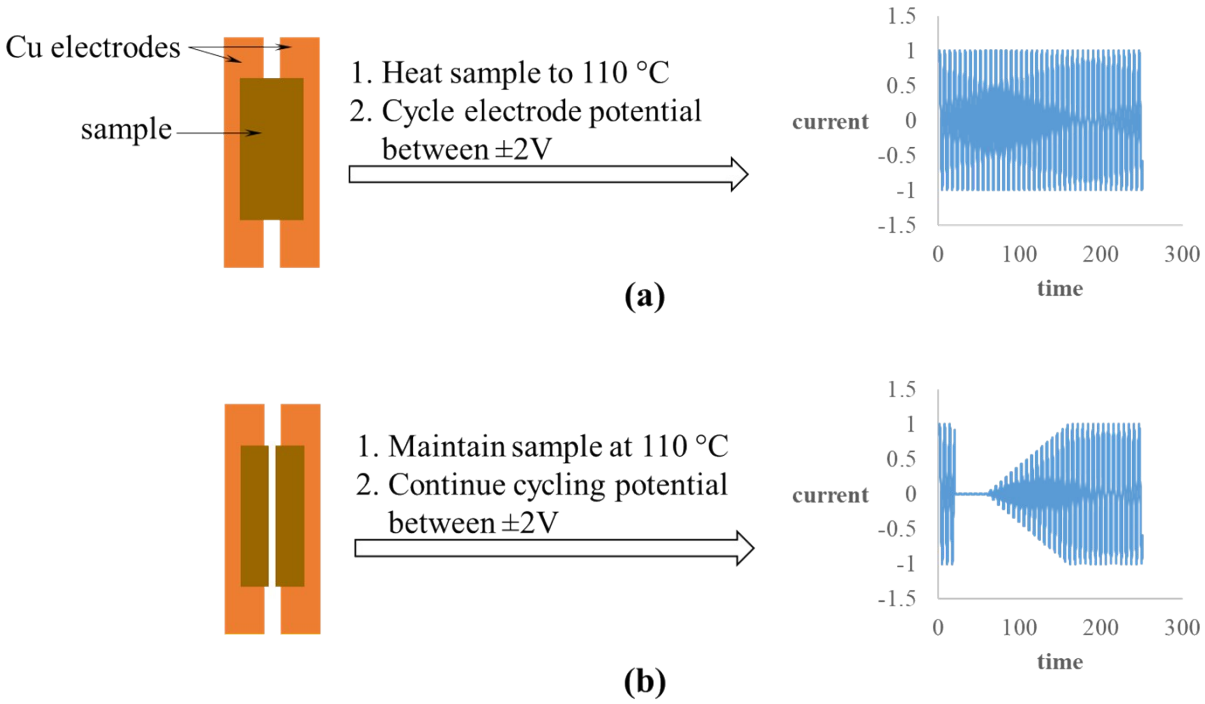


Figure S29: Steps taken to evaluate the recovery of polymer conductivity due to rehealing: (a) upon heating and cycling electrode potential, measured currents will stabilize at a consistent value, (b) once cut, the current will diminish substantially, then will begin to return/recover as the polymer heals.

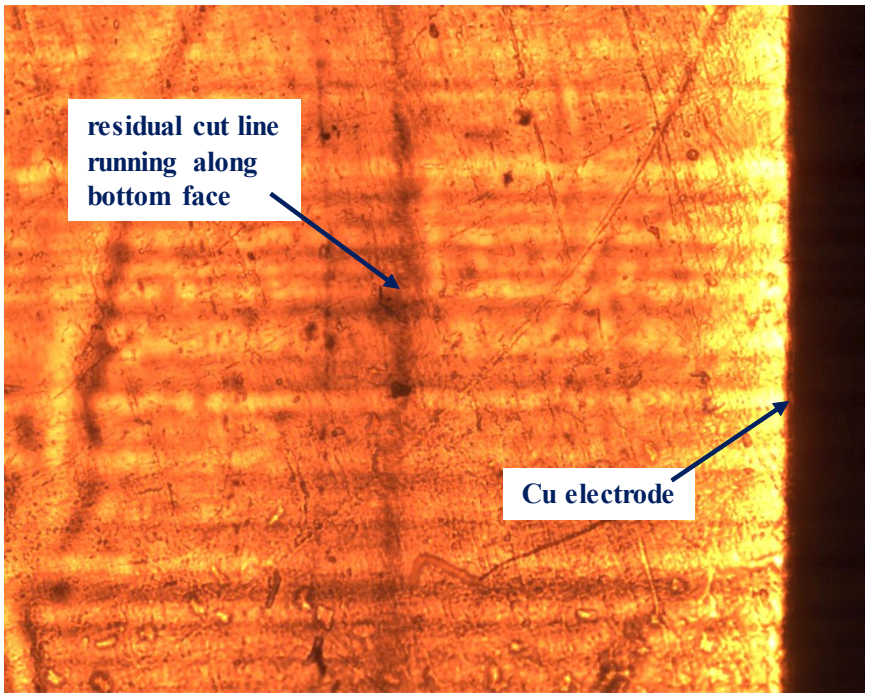


Figure S30: Microscopic image (10x magnification) of a sample subjected to a conductivity recovery experiment. The sample healed from the top to a depth of ~ 80%, which is why the remaining cut line along the bottom is well outside the focal plane and faint.

**References.**

1. J. Bara, Ind. Eng. Chem. Res., 2011, 50, 13614-13619.

2. Y. Cui, Y. Yan, Z. Wang, Macromol. Chem. Phys., 2013, 214, 470-477.

3. K. Yang, J. C. Grant, P. Lamey, A. Joshi-Imre, B. R. Lund, R. A. Smaldone, W. Voit, Adv. Funct. Mater., 2017, 27, 1700318.

4. B. B. Jing, C. M. Evans, J. Am. Chem. Soc., 2019, 141, 18932.